



# Propionate functions as a feeding state–dependent regulatory metabolite to counter proinflammatory signaling linked to nutrient load and obesity

Kim Han,<sup>1</sup> Allison M. Meadows,<sup>1,2</sup> Matthew J. Rodman,<sup>1</sup> Anna Chiara Russo,<sup>1</sup> Rahul Sharma,<sup>1</sup> Komudi Singh,<sup>1</sup>  Shahin Hassanzadeh,<sup>1</sup> Pradeep K. Dagur,<sup>3</sup> Rebecca D. Huffstutler,<sup>4</sup> Fynn N. Krause,<sup>2</sup> Julian L. Griffin,<sup>2,5</sup> Yvonne Baumer,<sup>6</sup>  Tiffany M. Powell-Wiley,<sup>6</sup> and Michael N. Sack<sup>1,4,\*</sup>

<sup>1</sup>Laboratory of Mitochondrial Biology and Metabolism, National Heart, Lung, and Blood Institute, National Institutes of Health, Room 5-3342, Bld 10-CRC, 10 Center Drive, Bethesda, MD 20817, United States

<sup>2</sup>Department of Biochemistry, University of Cambridge, Sanger Bld, 80 Tennis Ct Rd, Cambridge CB2 1GA, United Kingdom

<sup>3</sup>Flow Cytometry Core Facility, National Heart, Lung, and Blood Institute, National Institutes of Health, 10 Center Drive, Bethesda, MD 20892, United States

<sup>4</sup>Cardiovascular Branch, National Heart, Lung, and Blood Institute, National Institutes of Health, 10 Center Drive, Bethesda, MD 20892, United States

<sup>5</sup>Rowett Institute, School of Medicine, Medical Sciences and Nutrition, Foresterhill Campus, University of Aberdeen, Ashgrove Rd W, Aberdeen AB25 2ZD, United Kingdom

<sup>6</sup>Social Determinants of Obesity and Cardiovascular Risk Laboratory, National Heart, Lung, and Blood Institute, National Institutes of Health, 10 Center Drive, Bethesda, MD 20892, United States

\*Corresponding author: Laboratory of Mitochondrial Biology and Metabolism, National Heart, Lung, and Blood Institute, National Institutes of Health, 10 Center Drive, Building 10-CRC, Room 5-3342, Bethesda, MD 20892, United States. Email: [sackm@nih.gov](mailto:sackm@nih.gov)

## Abstract

Generally, fasting and refeeding confer anti- and proinflammatory effects, respectively. In humans, these caloric-load interventions function, in part, via regulation of CD4<sup>+</sup> T cell biology. However, mechanisms orchestrating this regulation remain incomplete. We employed integrative bioinformatics of RNA sequencing and high-performance liquid chromatography–mass spectrometry data to measure serum metabolites and gene expression of peripheral blood mononuclear cells isolated from fasting and refeeding in volunteers to identify nutrient-load metabolite-driven immunoregulation. Propionate, a short chain fatty acid (SCFA), and the SCFA-sensing G protein–coupled receptor 43 (*ffar2*) were coordinately and inversely regulated by fasting and refeeding. Propionate and free fatty acid receptor agonists decreased interferon- $\gamma$  and interleukin-17 and significantly blunted histone deacetylase activity in CD4<sup>+</sup> T cells. Furthermore, propionate blunted nuclear factor  $\kappa$ B activity and diminished interleukin-6 release. In parallel, propionate reduced phosphorylation of canonical T helper 1 (T<sub>H</sub>1) and T<sub>H</sub>17 regulators, STAT1 and STAT3, respectively. Conversely, knockdown of free fatty acid receptors significantly attenuated the anti-inflammatory role of propionate. Interestingly, propionate recapitulated the blunting of CD4<sup>+</sup> T<sub>H</sub> cell activation in primary cells from obese individuals, extending the role of this metabolite to a disease associated with low-grade inflammation. Together, these data identify a nutrient-load responsive SCFA–G protein–coupled receptor linked pathway to regulate CD4<sup>+</sup> T<sub>H</sub> cell immune responsiveness.

**Keywords:** CD4<sup>+</sup> T cells, fasting, FFAR2, IL-6, metabolite, NF $\kappa$ B, propionate

## 1. Introduction

Fasting can be employed as an acute nutritional intervention to explore mechanisms linked to the health benefits of intermittent fasting, time-restricted eating, and other caloric-restrictive dietary strategies.<sup>1,2</sup> An emerging concept arising from these dietary interventions is that short-term or intermittent fasting confers anti-inflammatory effects in animal models and human studies<sup>3,4</sup> and that refeeding may be proinflammatory.<sup>1,5</sup> Mechanisms underpinning these immunoregulatory effects are being uncovered at the level of immune cell chromatin remodeling<sup>6,7</sup>; transcriptional control<sup>2</sup>; posttranslational regulation<sup>1</sup>; intracellular signal transduction,<sup>8</sup> via intracellular organelle effects, e.g. by altering mitochondrial fidelity or autophagy<sup>8</sup>; and directly through metabolic remodeling.<sup>9</sup> Additional immune cell extrinsic paracrine regulatory factors include the effects of nutritional restriction on the release of metabolites or regulatory proteins from nutrient-responsive organs such as adipose tissue, the liver, and skeletal muscle<sup>10–12</sup>; modification of the gut microbiome<sup>13</sup>; and

modulation of immune cell trafficking to and from the bone marrow niche.<sup>5,11,14</sup>

Canonical metabolites released from nutrient-sensing organs or modulated via the gut microbiome confer immune regulatory effects, including synthesis of ketone bodies, predominantly from the liver, release of fatty acids and arachidonic acid from adipose tissue, and production and secretion of short-chain fatty acids (SCFAs) derived from the gut microbiome. The effects of ketone bodies are most well characterized, and different intermediates appear to confer distinct effects. This was illustrated in which  $\beta$ -hydroxybutyrate (BHB) and not acetoacetate attenuates the NLRP3 inflammasome in human and murine monocytes.<sup>15</sup> This effect of BHB occurs via disruption of the inflammasome complex formation but independent of BHB oxidation or activation of the BHB G protein–coupled receptor (GPR109A) or HCAR2 (hydrocarboxylic acid receptor 2).<sup>15</sup> In contrast, the initial exploration of the role of ketogenesis in neutrophils in response to the conditional genetic disruption of this pathway did not itself show a profound effect in the NLRP3-dependent

**Received:** June 14, 2023. **Revised:** December 18, 2023. **Accepted:** December 22, 2023. **Corrected and Typeset:** February 7, 2024

Published by Oxford University Press on behalf of Society for Leukocyte Biology 2024.

This work is written by (a) US Government employee(s) and is in the public domain in the US.

inflammasome, although neutrophil immune reactivity was ameliorated.<sup>16</sup> Interestingly, acetoacetate confers divergent immunoregulatory effects, including regulating human neutrophil migration,<sup>17</sup> blunting murine neuroinflammation,<sup>18</sup> and inducing NLRP3 activation of bovine mononuclear cells.<sup>19</sup> At the same time, gut microbiome-generated SCFAs have been identified as immunomodulatory metabolites.<sup>20</sup> For example, butyrate (C4 SCFA) functions as a histone deacetylase inhibitor<sup>21</sup> and blunts NLRP3 activation in adipocytes,<sup>22</sup> and gut microbiome-generated propionate (C3 SCFA) reduces gut resident  $\gamma\delta$ T cell interleukin (IL)-17 production in mice and circulating  $\gamma\delta$ T cells in patients with inflammatory bowel disease.<sup>23</sup> Propionate has also been shown to augment the regulatory T (Treg)/T helper 17 (T<sub>H</sub>17) ratio<sup>24</sup> and blunt T<sub>H</sub>17-linked autoimmunity.<sup>25</sup> Similarly, both butyrate and propionate dampen the inflammatory activity and interferon- $\gamma$  (IFN $\gamma$ ) release from transformed dendritic epidermal T cells.<sup>26</sup> Together, these data support the role of circulating metabolites in immunoregulation and highlight divergent effects in different species and immune cell lineages.

Our laboratory has used fasting and refeeding as a human model system to further explore the biology of nutrient load-dependent immunomodulation. In an initial myeloid cell-focused study in healthy volunteers, we showed that a 24-h fast blunted the NLRP3 inflammasome in monocytes and macrophages and that refeeding after the 24-h fast exacerbated the NLRP3 inflammasome via nuclear factor  $\kappa$ B (NF- $\kappa$ B) activation.<sup>1</sup> A subsequent broad bioinformatics-driven study investigating peripheral blood mononuclear cells (PBMCs) extracted during fasting and refeeding identified nutrient load-dependent CD4<sup>+</sup> T cell regulation by concordant high-dimensional flow cytometric phenotyping and RNA sequencing analysis.<sup>2</sup> Functional characterization of these findings identified that CD4<sup>+</sup> T<sub>H</sub> cells exhibited a dampened immune responsiveness in the fasted relative to refed state. A subsequent integrated bioinformatics approach incorporating RNA sequencing and metabolomic and lipidomic analysis identified a novel fasting-induced metabolite, N-arachidonylglycine, linked to an orphan G protein-coupled receptor (GPCR), GPR18, that blunted T<sub>H</sub>1 and T<sub>H</sub>17 cell immune responsiveness in healthy individuals and cells extracted from obese subjects.<sup>27</sup> In that same study, the transcript level of the free fatty acid receptor 2 (FFAR2) (GPR43), which is activated by SCFAs, was found to be induced in the refed state.<sup>27</sup> The objective of this study was to evaluate whether 24-h fasting and refeeding modulated SCFAs and whether these putative microbiome-derived lipids have direct nutrient state-dependent CD4<sup>+</sup> T<sub>H</sub> cell immunomodulatory effects.

In this study, we find that propionate levels, compared with acetate and butyrate, are increased in the refed relative to the fasting state. This is paralleled by increased FFAR2 and FFAR3 (GPR41) expression in CD4<sup>+</sup> T cells following refeeding. Subsequent biochemical, pharmacologic, and genetic manipulation of the propionate-FFAR pathways uncover that propionate attenuates T<sub>H</sub>1 and T<sub>H</sub>17 immune responsiveness via downregulation of histone deacetylase (HDAC) activity with subsequent blunting of NF- $\kappa$ B, IL-6, STAT1, and STAT3 signal transduction. Together, these data show that propionate functions as a negative regulator of CD4<sup>+</sup> T cell immune responsiveness in the refed state.

## 2. Methods

### 2.1 Clinical protocol

To further characterize pathways that orchestrate nutrient-dependent immune modulation, we carried out a clinical study (<https://classic.clinicaltrials.gov/ct2/show/NCT02719899>) to assess

the immunologic effects of a 24-h fast and a period of refeeding on PBMCs in normal volunteers which has previously been described by Han et al.<sup>2</sup> The National Heart, Lung, and Blood Institute Institutional Review Board approved this study, and volunteers signed informed consent before participation. Females (n = 11) and males (n = 10) 22 to 29 yr of age with no acute or chronic disease and a body mass index (BMI) weight range of 22 to 29 kg/m<sup>2</sup> were recruited for the study. Volunteers fasted overnight (t = 0 h [baseline]), consumed a fixed 500-calorie morning meal, completed a 24-h total fast (t = 24 h [fasted]), then consumed another 500-calorie meal after the fast (t = 27 [refed]). The fixed 500-calorie meals consisted of a choice of either (meal 1) a vegetable omelet, toast with butter and jelly, and orange juice, or (meal 2) oatmeal with walnuts, brown sugar, dried cranberries, and milk. The schematic of the study design and the subject's characteristics are described in [Supplementary Fig. 1A](#). Primary CD4<sup>+</sup> T cells from lean and obese subjects were collected under the Disease Discovery Natural History Protocol (<https://classic.clinicaltrials.gov/ct2/show/NCT01143454>). Thirty African American female volunteers 24 to 78 yr of age were recruited for this study. Fifteen volunteers with an average BMI of 24.17  $\pm$  2.17 kg/m<sup>2</sup> and an average age of 53.73  $\pm$  18.49 yr were classified as lean. Fifteen volunteers with an average BMI of 40.29  $\pm$  8.06 kg/m<sup>2</sup> and an average age of 53.00  $\pm$  12.45 yr were classified as obese. Characteristics of lean and obese subjects are described in the results section. The blood from healthy volunteers for functional study was obtained from subjects that consented to enroll in the Disease Discovery Protocol (<https://classic.clinicaltrials.gov/ct2/show/NCT01143454>) and from the National Institutes of Health Clinical Center blood bank (<https://classic.clinicaltrials.gov/ct2/show/NCT00001846>).

### 2.2 Targeted detection of SCFAs in human serum

Serum samples from baseline, 24-h fasted, and 3-h refed states were extracted using a standard methanol-chloroform-water method.<sup>28</sup> The extracted aqueous fraction was derivatized with 33NPH•HCL to convert SCFAs to their corresponding 3-nitrophenylhydrazones using the method described by Han et al.<sup>29</sup> Derivatized samples were reconstituted in an internal standard solution containing the following 9 SCFAs, which had been derivatized with <sup>13</sup>C<sub>6</sub>-3NPH•HCL: acetic acid, propionic acid, isobutyric acid, butyric acid, isovaleric acid, valeric acid, isocaproic acid, caproic acid, and heptanoic acid. Targeted liquid chromatography/mass spectrometry was performed with a Thermo Scientific Vanquish UHPLC<sup>+</sup> coupled to a TSQ Quantiva mass spectrometer (Thermo Fisher Scientific). An ACE Excel 2 C18 PFP (100A, 150  $\times$  2.1 mm 5  $\mu$ m) column conditioned at 40  $^{\circ}$ C was used for chromatography with a mobile phase consisting of (1) a 0.1% formic acid solution in water and (2) a 0.1% formic acid solution in acetonitrile. The ESI source was operated in negative mode with an electrospray voltage of 2500 V, and nitrogen at 48 mTorr and 338  $^{\circ}$ C was used as a drying gas for solvent evaporation. Data were acquired and processed using Thermo Xcalibur software (Version 2.2; Thermo Fisher Scientific). Individual peaks were integrated and normalized to their corresponding internal standard.

### 2.3 Metabolomics analysis

SCFA data were compiled with metabolite and lipid data previously collected from identical fasting and refeeding serum samples for further analysis.<sup>27</sup> Supervised analysis was performed with orthogonal partial least squares discriminant analysis (OPLS-DA) using Simca software (version 17; Umetrics). Model performance

was reported using R2X, which represents variation in data explained by the model; R2Y, which explains variation in class membership explained by the model; and Q2, which describes the predictive capacity of the model. Significance testing was performed with cross-validation analysis of variance (ANOVA). Variables important for prediction (VIPs) were reported for the OPLS-DA model (Supplementary Table 1), and a heatmap of relative expression was generated using GraphPad Prism (version 9; GraphPad Software).

## 2.4 Transcriptomics analysis

RNA sequencing of PBMCs isolated from human volunteers that underwent the 24-h fasting and refeeding study was performed as previously described.<sup>2</sup> Data were accessed from the Gene Expression Omnibus repository (GEO ID: GSE165149).

## 2.5 Primary CD4<sup>+</sup> T cells isolation from whole blood

Primary PBMCs were isolated from human blood by density centrifugation using Lymphocyte Separation Medium (MP Biomedicals). CD4<sup>+</sup> T cells were negatively selected from PBMCs using the CD4<sup>+</sup> T Cell Isolation Kit (Miltenyi Biotec) and cultured in RPMI 1640 media supplemented with 25 mM HEPES, 10% heat-inactivated fetal bovine serum (FBS), and penicillin/streptomycin. Human CD4<sup>+</sup> T cells ( $4 \times 10^5$ /well in 96-well plate) were activated with plate-coated  $\alpha$ CD3 (5  $\mu$ g/mL; BioLegend) and  $\alpha$ CD28 (10  $\mu$ g/mL; BioLegend) for 3 d in the presence of 10% autologous serum from the subjects and 5% FBS. Also, CD4<sup>+</sup> T cells ( $4 \times 10^5$ /well in a 96-well plate) were differentiated into 3 T cell subtypes by incubation with the specific supplements for T<sub>H</sub>1 (20 ng/mL IL-12 and 10  $\mu$ g/mL  $\alpha$ IL-4), T<sub>H</sub>2 (10 ng/mL IL-4 and 10  $\mu$ g/mL  $\alpha$ IFN $\gamma$ ), or T<sub>H</sub>17 (20 ng/mL IL-6, 2 ng/mL transforming growth factor  $\beta$ 1, 10 ng/mL IL-1 $\beta$ , 10 ng/mL IL-23, 10  $\mu$ g/mL  $\alpha$ IL-4, and 10  $\mu$ g/mL  $\alpha$ IFN $\gamma$ ), respectively. They were differentiated for 3 d on plate-coated  $\alpha$ CD3 and  $\alpha$ CD28 in the presence of 10% autologous serum from the subjects and 5% FBS. All recombinant proteins and antibodies for differentiation media were purchased from PeproTech and eBioscience. Supernatants were collected, centrifuged to remove cells and debris, and stored at  $-80^\circ\text{C}$ .

## 2.6 Flow cytometry

CD4<sup>+</sup> T cells were isolated from healthy volunteers and incubated with 5 mM propionate for 3 d on plate-coated  $\alpha$ CD3 and  $\alpha$ CD28. The cells were activated with a Cell Stimulation Cocktail (plus protein transport inhibitors) (eBioscience) and PMA (500 ng/mL; Sigma) for 4 h and then incubated with antibodies against cell surfaces and cytokines (BD, BioLegend, eBioscience) (Supplementary Table 2)). Data were acquired with FACSymphony (BD), and post-acquisition analysis was performed using FlowJo 9.9.6 (TreeStar). Analysis excluded debris and doublets using light scatter measurements and dead cells by live/dead stain. Gating strategies used to identify immune cell subsets are provided in Supplementary Figs. 1F and 2H. Briefly, the cells were first gated for singlets (forward scatter height [FSC-H] vs forward scatter area [FSC-A]) and further analyzed for their uptake of the Live/Dead Yellow stain (Invitrogen) to determine live vs dead cells in CD8<sup>-</sup>CD4<sup>+</sup> or CD3<sup>+</sup>CD4<sup>+</sup>. The expression of transcription factors and cytokines is then determined for T cell polarization within this gated population.

## 2.7 Treatment with metabolites and receptor ligands

CD4<sup>+</sup> T cells were treated with propionate (C3), 4CMTB (FFAR2 agonist; Tocris Bioscience), AR420626 (FFAR3 agonist; Tocris Bioscience), or GLPG0974 (FFAR2 antagonist; Tocris Bioscience) on  $\alpha$ CD3/ $\alpha$ CD28 antibody-coated plates for 3 d. Cytotoxicity was assessed using the Vibrant MTT cell proliferation assay (Thermo Fisher Scientific) and CyQUANT LDH Cytotoxicity Assay (Invitrogen). On the third day, cells were centrifuged for Western blot or RNA analysis and the supernatant was collected for enzyme-linked immunosorbent assay (ELISA) assay.

## 2.8 Characterization of propionate signaling in primary human T cells

Primary CD4<sup>+</sup> T cells with 5 mM propionate were cultured in RPMI with 1% FBS on  $\alpha$ CD3/ $\alpha$ CD28 antibody-coated plates for 3 d. The following activators or antibodies were added to propionate-treated cells in parallel for 24 h: the NF- $\kappa$ B activator betulinic acid (BA) (10  $\mu$ M; Tocris Bioscience), the JAK/STAT activator RGCD423 (5  $\mu$ M; Tocris Bioscience), or  $\alpha$ IL6-neutralizing monoclonal antibody (1  $\mu$ g/mL; Invivogen). Cytotoxicity was assessed using the CyQUANT LDH Cytotoxicity Assay (Invitrogen). NF- $\kappa$ B RelA/p65 Transcription Factor Activity Assay Kit (Abcam) and HDAC Cell-Based Activity Assay Kit (Cayman Chemical) were used to measure NF- $\kappa$ B p65 activity and HDAC activity, respectively. CD4<sup>+</sup> T cells were incubated with propionate, 4CMTB, or AR420626 for 48 h and BA, HDAC inhibitor trichostatin A (TSA) (10  $\mu$ M; Selleck Chemicals), or ITF2357 (200 nM; Selleck Chemicals) for 24 h. Further, 10  $\mu$ g protein extracts were used for NF- $\kappa$ B activity assay according to the manufacturer's protocol. For HDAC activity assay, TSA (2.1  $\mu$ M) or ITF2357 (500 nM) was treated for 2 h and then processed to measure the HDAC activity of the reagents according to the manufacturer's protocol. HDAC activity was calculated using the equation obtained from the linear regression of the standard curve, substituting collected fluorescence values for each sample. HDAC activity (nmol/min/mL) = [(non-TSA sample fluorescence—TSA sample fluorescence)—(y-intercept)/slope]/15 min.

## 2.9 Genetic knockdown experiments

For the small interfering RNA (siRNA) knockdown experiments, primary CD4<sup>+</sup> T cells were transfected with 1.5  $\mu$ M SMARTpool Accell FFAR2 and FFAR3 siRNA or Accell control siRNA in Accell siRNA delivery medium (Dharmacon). Accell media was supplemented with 2% FBS. Cells were treated with 5 mM propionate and activated on  $\alpha$ CD3/ $\alpha$ CD28 antibody-coated plates for 3 d.

## 2.10 ELISA immunoassay

After activation and treatment, cell supernatants were collected for cytokine assay, and cell pellets were reserved for normalization. The cytokines IFN $\gamma$ , IL-4, IL-5, IL-6 and IL-17 were measured by ELISA kits (R&D Systems), and results were collected using a microplate reader. Cytokine levels were normalized to cell density using the CyQUANT Cell Proliferation Assay (Invitrogen) or the bicinchoninic acid protein assay (Pierce).

## 2.11 Immunoblot analysis

Protein was extracted from CD4<sup>+</sup> T cells in RIPA buffer containing 50 mM of Tris-HCl (pH 8.0), 0.5% deoxycholic acid, 1% NP-40, 0.1% sodium dodecyl sulfate, and 0.5 M NaCl (Boston BioProducts) supplemented with protease and phosphatase inhibitors (Pierce). Protein concentration was measured using the bicinchoninic



acid protein assay (Pierce). Lysates were separated by NuPAGE 4% to 12% Bis-Tris Protein Gels (Thermo Fisher Scientific) and transferred to nitrocellulose membranes (Trans-Blot Turbo Transfer System; Bio-Rad Laboratories). Membranes were blocked with Odyssey Blocking Buffer (Li-Cor Biosciences) and incubated with appropriate antibodies. Primary antibodies for each steady-state protein and associated phosphoprotein STAT1 and pSTAT1 (Y701), STAT3 and pSTAT3 (Y705), STAT6 and pSTAT6 (Y641), NF $\kappa$ B-p65 and pNF $\kappa$ B-p65 (S536), and pl $\kappa$ B $\alpha$  (S32) were provided by Cell Signaling Technology. Antibodies against FFAR2 and FFAR3 were purchased by Sigma and Millipore, respectively. Actin (Millipore) was used as a loading control. Immunoblots were scanned using an Odyssey Clx imaging system (Li-Cor Biosciences), and protein band intensity was quantified using Image Studio software (version 5.2; Li-Cor Biosciences).

## 2.12 Quantitative real-time polymerase chain reaction

RNA was isolated from CD4<sup>+</sup> T cells using the NucleoSpin RNA kit (Macherey-Nagel). Complementary DNA was synthesized using the SuperScript III First-Strand Synthesis kit (Invitrogen). Quantitative real-time polymerase chain reaction was prepared using the SYBR Green FastStart Essential DNA Master Mix (Roche) and performed on a LightCycler 96 (version 1.1; Roche). The primers of canonical transcription factors of CD4<sup>+</sup> T cell were made by Integrated DNA Technologies, and the sequences of the primers are listed: TBX21 (T-bet, F: CGTGACTGCCTACCAG AAT and R: ATCTCCCCAAGGAATTGAC), GATA3 (F: GAACCGG CCCCTCATTAAG and R: ATTTTTCGGTTTCTGGTCTGGAT), RORC (ROR $\gamma$ t, F: GCATGTCCCGAGATGCTGTC and R: CTGGGAGCCCC AAGGTGTAG), and EF1 $\alpha$  (F: GTTGATATGGTTCCTGGCAAGC and R: GCCAGCTCCAGCAGCCTTC). The following human gene-specific QuantiTect primer assays (Qiagen) were used: FFAR2 (QT00214473), FFAR3 (QT00214956), IL-6 (QT00083720), and 18S (QT00199367). Relative gene expression was quantified by normalizing cycle threshold values with 18S rRNA for FFAR2, FFAR3, and IL-6 and with EF1 $\alpha$  for TBX21, GATA3, and RORC using the 2<sup>- $\Delta\Delta$ Ct</sup> cycle threshold method.

## 2.13 Graphing and statistics

Graphing and statistical interpretation of data were performed in GraphPad Prism (version 9). The number of biological replicates is reported as *n* in each figure legend, and each biological replicate was performed on cells isolated from a distinct whole blood sample. Each biological replicate represents the mean of technical replicates performed in duplicate. Dot plots contain every biological replicate, and error bars show the SEM. Parametric hypothesis testing was performed using a Student's *t* test when comparing 2 group means and an ANOVA with multiple comparisons test when comparing 3 or more group means. Statistical tests and resulting *P* values are reported in each figure legend.

## 3. Results

### 3.1 Propionate levels are nutrient-load dependent and differentially modulate T<sub>H</sub>1 and T<sub>H</sub>17 cell signaling

To identify potential immunomodulatory effects by nutrient load, we first employed targeted metabolomics to assess serum SCFA levels by comparing the baseline, 24-h fasted, and 3-h refed states (Supplementary Fig. 1A). The OPLS-DA of metabolomic and lipidomic data were distinctly separated between 3 groups ( $R^2X = 0.392$ ,

$R^2Y = 0.865$ ,  $Q^2 = 0.721$ , and cross-validation ANOVA  $P = 3.66 \times 10^{-22}$ ) and attributed to distinct fasting-mediated changes in the circulating plasma metabolome during fasting (Supplementary Fig. 1B). This OPLS-DA model was validated using a permutation plot (Supplementary Fig. 1C). Distinct metabolite biomarkers were identified using VIP. A total of 115 of the 245 differentially abundant metabolites had a VIP score >1 (Supplementary Table 1). Interestingly, of the SCFAs, only propionate (C3) showed a significant difference with elevated levels in the refed compared with baseline and fasted state (Fig. 1A). Additionally, we subdivided this clinical cohort into 2 isocaloric meal options chosen after 24-h fasting and compared circulating levels of C3. The differential release of C3 was shown only in subjects taking meal 1 (vegetable omelet, toast with butter and jelly, and orange juice) but not in subjects taking meal 2 (oatmeal with walnuts, brown sugar, dried cranberries, and milk) (Supplementary Fig. 1D). In contrast, acetate (C2), butyrate (C4), and valerate (C5) were unchanged comparing fasting to refeeding (Fig. 1B). In parallel, we interrogated the RNA sequencing database of PBMC samples from the same subjects (GSE165149).<sup>2</sup> Quantification of FFAR2 (GPR43) RNA sequencing analysis expression showed that this GPCR was upregulated in the refed state (mean fold change = 1.61, *P* value = 0.0071, *n* = 21) compared with fasting. Quantitative polymerase chain reaction of RNA from PBMCs from our initial fasting and refeeding study subjects confirmed that the levels of FFAR2 were significantly induced in the refed state, whereas FFAR3 (GPR41) transcript levels did not reach significance comparing the 3 nutritional states (Supplementary Fig. 1E). However, protein levels of FFAR2 and FFAR3 in PBMCs were increased in the refed state compared with the fasted state (Fig. 1C). CD4<sup>+</sup> T cells isolated from the same subjects showed that refeeding induced the transcript levels of both FFAR2 and FFAR3 (Fig. 1D). Given that CD4<sup>+</sup> T<sub>H</sub> cell responsiveness is differentially regulated in the fasted and refed states, we explored the effect of propionate supplementation on primary CD4<sup>+</sup> T cells extracted from healthy volunteers and assayed canonical T<sub>H</sub>1, T<sub>H</sub>2, and T<sub>H</sub>17 cytokines after T cell receptor (TCR) activation (activated CD4<sup>+</sup> T cells: T<sub>H</sub>0). Interestingly, only the T<sub>H</sub>1 and T<sub>H</sub>17 cytokines, namely IFN $\gamma$  and IL-17, were blunted by propionate, with no effects on the T<sub>H</sub>2 cytokine IL-4 (Fig. 1E, F and Supplementary Fig. 1F). CD4<sup>+</sup> T cells were then polarized into T<sub>H</sub>1, T<sub>H</sub>2, and T<sub>H</sub>17 cells with differentiation supplements, respectively, and here propionate had the greatest effect on attenuating IFN $\gamma$  and IL-17 secretion over that of T<sub>H</sub>2 cytokine IL-5 (Fig. 1G). Propionate was administered at 5 mM, which did not affect primary CD4<sup>+</sup> T cell viability (Supplementary Fig. 1G). Additionally, cytokine release of IFN $\gamma$  and IL-17 was attenuated down to a propionate dose of 10  $\mu$ M (Supplementary Fig. 1H).

### 3.2 FFAR2 and FFAR3 levels control CD4<sup>+</sup> T cell immune responsiveness

To begin to characterize how propionate modulates CD4<sup>+</sup> T<sub>H</sub> cell responsiveness, we assayed whether propionate directly modified FFAR2 and FFAR3 expression. Here, incubating primary CD4<sup>+</sup> T cells with propionate significantly increased protein levels of both these SCFA transporters (Fig. 2A). Furthermore, siRNA-targeted genetic knockdown of either of these GPCRs in CD4<sup>+</sup> T cells abolished propionate's ability to blunt IFN $\gamma$  and IL-17 release (Fig. 2B). Interestingly, knockdown of FFAR2/3 alone increased IFN $\gamma$  and IL-17 release (Fig. 2B). In these studies, the extent of FFAR2 or FFAR3 transcript knockdown achieved was ~40% in CD4<sup>+</sup> T cells (Supplementary Fig. 2A, B). Additionally, FFAR2 and FFAR3 agonist 4CMTB, but not AR420626, increased protein levels

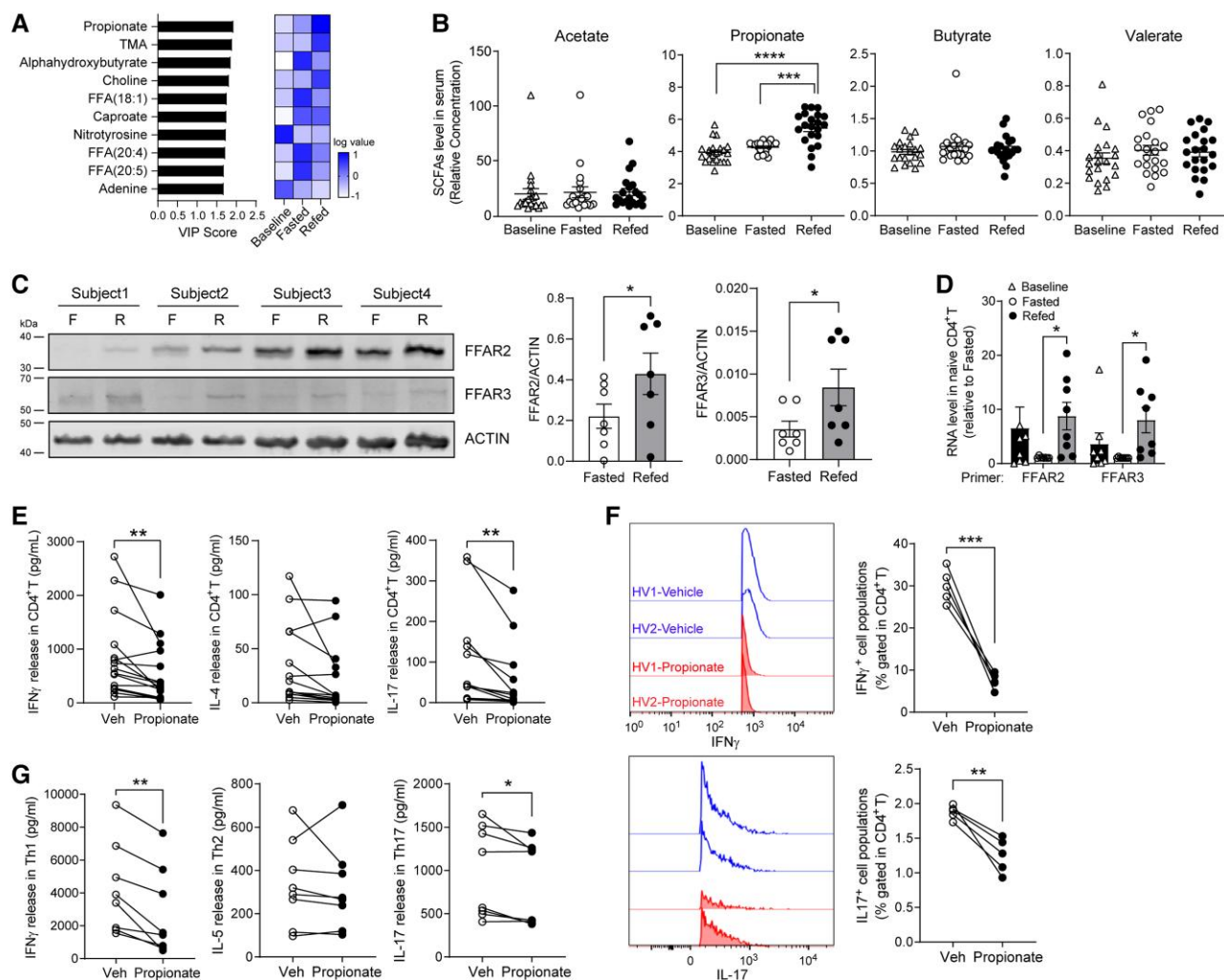


**Fig. 1.** Functional characterization of propionate signaling in CD4<sup>+</sup> T cells. (A) Top 10 VIPs and heatmap of mean log abundance in baseline, fasted, and refed serum samples. (B) Relative abundance of SCFAs (C2–C5) in serum collected from volunteers at 3 time points ( $n = 21$ ). Significance reported with a paired *t* test. Significance reported with a repeated measures 1-way ANOVA analysis. \*\*\*\* $P < 0.0001$ , \*\*\* $P < 0.001$ . Acetate (C2); propionate (C3); butyrate (C4); valerate (C5). (C) Protein expression of FFAR2 and FFAR3 in PBMCs ( $n = 7$ /group) collected at fasted (F) and refed (R) time points. Significance using a paired *t* test. \* $P < 0.05$ . (D) RNA expression of FFAR2 (GPR43) and FFAR3 (GPR41) in naive CD4<sup>+</sup> T cells ( $n = 8$ /group) collected at 3 time points (relative to the mean of fasted group). Gene expression values measured by quantitative real-time polymerase chain reaction and normalized to 18S. Significance using a 2-way ANOVA. \* $P < 0.05$ . (E) Release of IFN $\gamma$ , IL-4, and IL-17 cytokines from CD4<sup>+</sup> T cells treated with 5 mM propionate ( $n = 12$ –16). Cytokines measured by ELISA immunoassay and normalized to cell density by CyQuant assay. Significance reported using a paired *t* test. \*\* $P < 0.01$ . (F) Representative flow plots to show the cell population of IFN $\gamma$ <sup>+</sup> and IL-17<sup>+</sup> cells in propionate-treated CD4<sup>+</sup> T cells ( $n = 5$ ). Significance using a paired *t* test. \*\* $P < 0.01$ , \*\*\* $P < 0.001$ . (G) Release of IFN $\gamma$ , IL-5, and IL-17 cytokines from differentiated CD4<sup>+</sup> T cells treated with propionate relative to vehicle control ( $n = 8$ ). CD4<sup>+</sup> T cells were differentiated into 3 T cell subtypes by incubation with the specific supplements for T<sub>H</sub>1 (20 ng/mL IL-12 and 10  $\mu$ g/mL  $\alpha$ IL-4), T<sub>H</sub>2 (10 ng/mL IL-4 and 10  $\mu$ g/mL  $\alpha$ IFN $\gamma$ ) or T<sub>H</sub>17 (20 ng/mL IL-6, 2 ng/mL transforming growth factor  $\beta$ 1, 10 ng/mL IL-1 $\beta$ , 10 ng/mL IL-23, 10  $\mu$ g/mL  $\alpha$ IL-4, and 10  $\mu$ g/mL  $\alpha$ IFN $\gamma$ ), respectively. Cytokines measured by ELISA immunoassay and normalized by CyQuant assay. Significance reported using a paired *t* test. \* $P < 0.05$ , \*\* $P < 0.01$ . TMA = trimethylamine.

of FFAR2 and FFAR3 in CD4<sup>+</sup> T cells (Fig. 2C). Despite this, both agonists blunted IFN $\gamma$  and IL-17 secretion (Fig. 2D). Consistent with these immunomodulatory effects, FFAR2/3 agonists similarly blunted the cell populations labeled with the canonical transcription factors and cytokines driving T<sub>H</sub>1 (TBX21 [T-bet]<sup>+</sup>IFN $\gamma$ <sup>+</sup>) and T<sub>H</sub>17 (RORC [ROR $\gamma$ t]<sup>+</sup>IL17<sup>+</sup>) polarization (Fig. 2E) and the transcript level of TBX21 and RORC (Supplementary Fig. 2C). In parallel, the FFAR2 antagonist GLPG0974 reversed the effects of C3 on blunting IFN $\gamma$  and IL-17 release, T<sub>H</sub>1 (TBX21<sup>+</sup>IFN $\gamma$ <sup>+</sup>) and T<sub>H</sub>17 (RORC<sup>+</sup>IL17<sup>+</sup>) cell populations (Fig. 2F, G), and transcript level (Supplementary Fig. 2D). 4CMTB, AR420626, and GLPG0974 were administered at 10  $\mu$ M, which did not affect primary CD4<sup>+</sup> T cell viability (Supplementary Fig. 2E–G), and CD3<sup>+</sup>CD4<sup>+</sup> T cells were gated for measuring the T cell polarization in flow cytometry (Supplementary Fig. 2H).

### 3.3 Propionate attenuates NF- $\kappa$ B-mediated T<sub>H</sub>1 and T<sub>H</sub>17 polarization

SCFAs are known to signal via FFAR2/FFAR3 and to inhibit HDACs.<sup>30</sup> In parallel, HDAC inhibition confers anti-inflammatory effects by modulating T<sub>H</sub> cell polarization via targeting the IL-6 pathway in experimental colitis.<sup>31</sup> We therefore explored these putative signaling pathways linked to propionate orchestrated GPCR signaling. We show that propionate significantly blunted HDAC activity in CD4<sup>+</sup> T cells, and the FFAR agonists 4CMTB and AR420626 recapitulated this phenotype (Fig. 3A, B). ITF2357, an HDAC inhibitor, abolished the specific effect of C3 on HDAC activity (Fig. 3A, B). As HDAC inhibition is known to indirectly blunt NF- $\kappa$ B activation,<sup>32</sup> we assayed the effect of propionate on NF- $\kappa$ B phosphorylation and NF- $\kappa$ B binding activity to NF- $\kappa$ B consensus

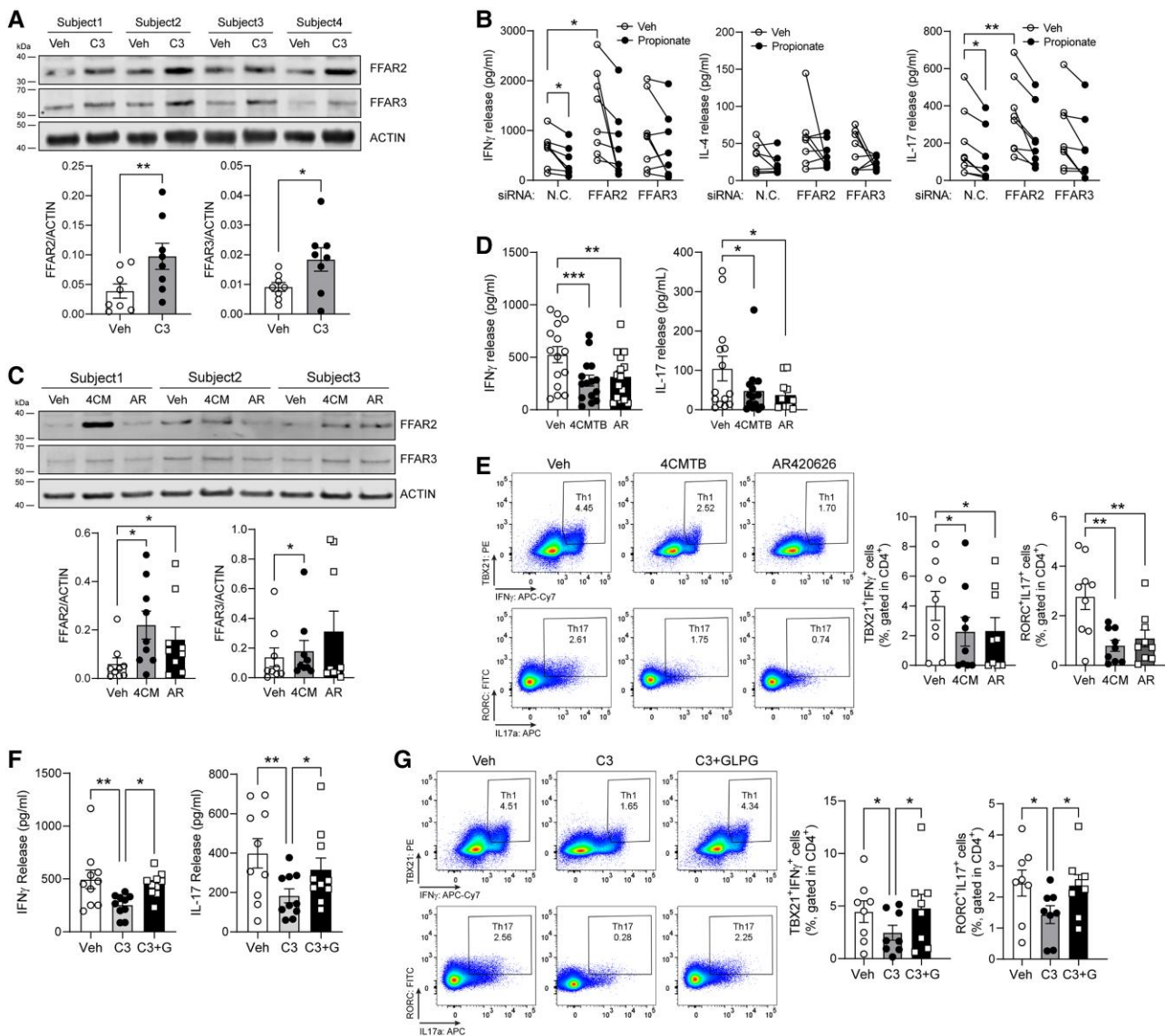


**Fig. 2.** Functional characterization of FFAR2 and FFAR3 in CD4<sup>+</sup> T cells. (A) Protein expression of FFAR2 and FFAR3 in CD4<sup>+</sup> T cells treated with propionate relative to vehicle groups (n = 8). Significance reported using a paired t test. \*P < 0.05, \*\*P < 0.01. (B) Release of IFN $\gamma$ , IL-4, and IL-17 cytokines from CD4<sup>+</sup> T cells treated with FFAR2 siRNA or FFAR3 siRNA response to propionate (n = 8). Cytokines measured by ELISA immunoassay and normalized to cell density by CyQuant assay. Significance reported using a 2-way ANOVA with Šidák's multiple comparisons test. \*P < 0.05, \*\*P < 0.01. (C) Protein expression of FFAR2 and FFAR3 in CD4<sup>+</sup> T cells treated with 10  $\mu$ M 4CMTB (4CM) (FFAR2 agonist) or 10  $\mu$ M AR420626 (AR) (FFAR3 agonist) relative to vehicle groups (n = 9). Significance reported using a 1-way ANOVA with Šidák's multiple comparisons test. \*P < 0.05. (D) Cytokine release of IFN $\gamma$  and IL-17 from CD4<sup>+</sup> T cells treated with 4CMTB or AR. Significance reported using a 1-way ANOVA with Dunnett's multiple comparisons test (n = 9–10). \*P < 0.05, \*\*P < 0.01, \*\*\*P < 0.001. (E) Representative flow plots to show the cell population of Th1 (TBX21<sup>+</sup> IFN $\gamma$ <sup>+</sup> gated in CD4<sup>+</sup>) and Th17 (RORC<sup>+</sup> IL17<sup>+</sup> gated in CD4<sup>+</sup>) in CD4<sup>+</sup> T cells treated with 4CMTB or AR relative to vehicle groups (n = 9). Significance reported using a 1-way ANOVA with Dunnett's multiple comparisons test. \*P < 0.05, \*\*P < 0.01. (F) Cytokine release of IFN $\gamma$  and IL-17 from CD4<sup>+</sup> T cells treated with C3 and FFAR2 antagonist, GLPG0974 (G, 10  $\mu$ M). Significance reported using a repeated measures 1-way ANOVA with Šidák's multiple comparisons test (n = 10). \*P < 0.05, \*\*P < 0.01. (G) Representative flow plots to show the cell population of Th1 (TBX21<sup>+</sup> IFN $\gamma$ <sup>+</sup> gated in CD4<sup>+</sup>) and Th17 (RORC<sup>+</sup> IL17<sup>+</sup> gated in CD4<sup>+</sup>) in CD4<sup>+</sup> T cells treated with C3 and GLPG0974 (G) relative to vehicle groups (n = 8). Significance reported using a repeated measures 1-way ANOVA with Šidák's multiple comparisons test. \*P < 0.05. Veh = vehicle.

oligonucleotides. Propionate blunted NF- $\kappa$ B phosphorylation and binding activity, and the NF- $\kappa$ B activator BA reversed this phenotype (Fig. 3C, D). CD4<sup>+</sup> T cells treated with BA alone had slightly increased NF- $\kappa$ B binding activity (Supplementary Fig. 3A) and Th1 and Th17 polarization (Supplementary Fig. 3B). Also, 4CMTB and AR420626 replicated the blunting of NF- $\kappa$ B signaling activity (Fig. 3E, F). In parallel, inhibition of HDAC activity using TSA and ITF2357 (ITF) both phenocopied the C3 effect in attenuating IFN $\gamma$  and IL-17 cytokine release and NF- $\kappa$ B binding activity (Supplementary Fig. 3C, D).

### 3.4 IL-6 signaling is a component of propionate-mediated dampening of T cell activation

NF- $\kappa$ B, via its transactivation of IL-6, is known to phosphorylate and activate lineage-distinct STAT regulatory proteins controlling CD4<sup>+</sup> Th cell fate.<sup>33,34</sup> This pathway was assessed in response to C3 supplementation in Th0 cells. Here, C3 blunted both the transcript encoding IL-6 and IL-6 secretion from Th0 cells, and the NF- $\kappa$ B activator BA reversed these C3 effects (Fig. 4A, B). Furthermore, inhibition of HDAC activity using TSA and ITF phenocopied the C3 effect by reducing IL-6 secretion (Supplementary Fig. 4A, B). In



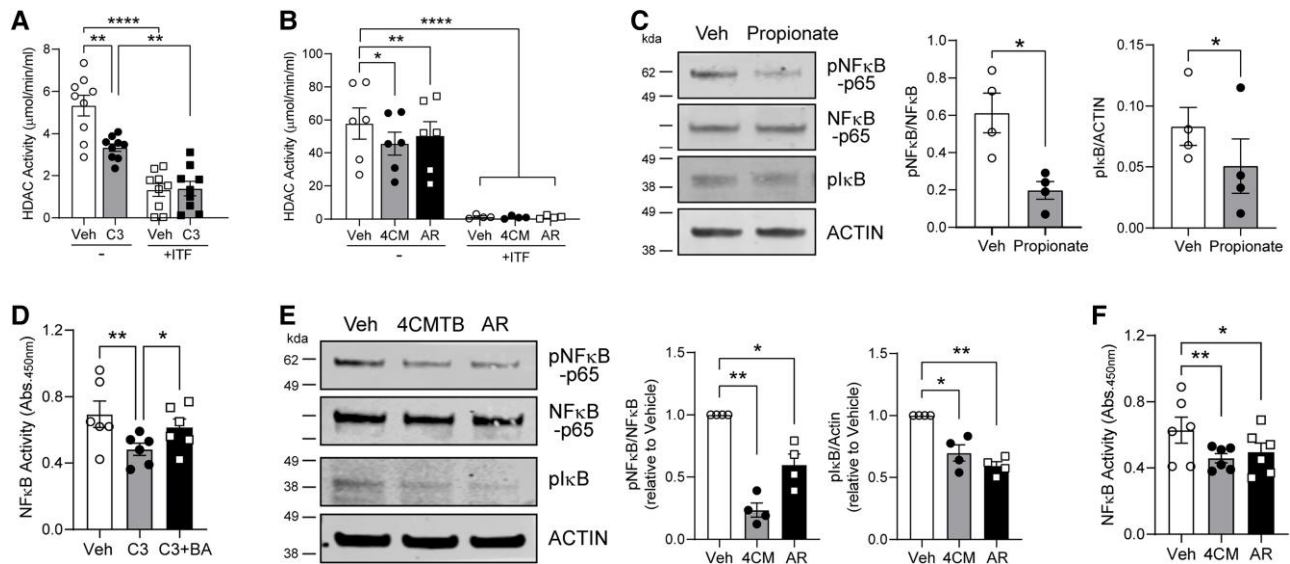


**Fig. 3.** HDAC inhibition by propionate regulates CD4<sup>+</sup> T cell polarization. (A) HDAC activity in CD4<sup>+</sup> T cells with 5 mM propionate for 48 h and 2.1 μM TSA (HDAC inhibitor) or 500 nM ITF2357 (ITF) (HDAC inhibitor) for 2 h. HDAC activity was calculated using the equation obtained from the linear regression of the standard curve, substituting collected fluorescence values for each sample. HDAC activity (nmol/min/mL) = [(non-TSA sample fluorescence—TSA sample fluorescence)—(y-intercept)/slope]/15 min. Significance reported using a 1-way ANOVA with Šidák's multiple comparisons test (n = 9). \*\*P < 0.01, \*\*\*P < 0.001. (B) HDAC activity in CD4<sup>+</sup> T cells with 10 μM 4CMTB (4CM) (FFAR2 agonist) or 10 μM AR420626 (AR) (FFAR3 agonist) for 48 h and TSA or ITF for 2 h. Significance reported using a repeated measures 1-way ANOVA with Dunnett's multiple comparisons test (n = 6). \*P < 0.05, \*\*P < 0.01, \*\*\*P < 0.001. (C) Immunoblot of NF-κB phosphoprotein abundance in CD4<sup>+</sup> T cells treated with propionate relative to vehicle control. Quantification of immunoblot: pNFκB/NFκB-p65 and pIκB/ACTIN. Significance reported using a paired t test. \*P < 0.05 (n = 4). (D) NF-κB activity in CD4<sup>+</sup> T cells with propionate and combination of NF-κB activator, BA. Active NFκB-p65 present in the protein extract specifically binds to the immobilized NFκB-p65 consensus binding site. Binding activity was measured by absorbance at 450 nm. Significance reported using a 1-way ANOVA with Šidák's multiple comparisons test. \*P < 0.05, \*\*P < 0.01 (n = 6). (E) Immunoblot image and quantification in FFAR2/FFAR3 agonist-treated CD4<sup>+</sup> T cells by TCR activation (n = 4). Significance reported using a repeated measures 1-way ANOVA with Dunnett's multiple comparisons test. \*P < 0.05, \*\*P < 0.01. (F) NF-κB activity in CD4<sup>+</sup> T cells with 4CMTB or AR. Active NFκB-p65 present in the protein extract specifically binds to the immobilized NFκB-p65 consensus binding site. Significance reported using a 1-way ANOVA with Tukey's multiple comparisons test (n = 6). \*P < 0.05, \*\*P < 0.01. Veh = vehicle.

parallel, C3 blunted the phosphorylation of STAT1 and STAT3 but not of STAT6 (Fig. 4C), and the FFAR2 and FFAR3 agonists mirrored the blunting effect of C3 on IL-6 release and STAT1/3 phosphorylation (Fig. 4D–F). In contrast, FFAR2 antagonist GLPG0974 reversed the effects of C3 on blunting IL-6 release (Supplementary Fig. 4C). The hierarchy of this signaling pathway was confirmed where the suppression of IFN $\gamma$  and IL-17 secretion in response to C3 was abrogated by the NF- $\kappa$ B activator BA (Fig. 4G). In parallel, the inhibition of IL-6 employing an IL-6 neutralizing antibody ( $\alpha$ IL-6) reversed the effect of NF $\kappa$ B activation in the presence of C3 (Fig. 4G). Furthermore, stimulation of the IL-6 receptor signaling with the glycoprotein 130 modulator RCGD423 similarly reversed the C3 effects on IFN $\gamma$  and IL-17 release (Fig. 4H). The proposed NF- $\kappa$ B pathway in response to propionate stimulation is shown in Supplementary Fig. 4D.

### 3.5 Anti-inflammatory effects of propionate are operational in obesity

Finally, we explored whether C3 could ameliorate immune responsiveness in an inflammation-linked condition. As obesity is known to exhibit both increased T<sub>H</sub>1- and T<sub>H</sub>17-mediated inflammation<sup>35,36</sup> and immune modulatory changes associated with fasting and refeeding may be relevant to the inflammatory pathophysiology of metabolic disease,<sup>10</sup> we compared the response of primary CD4<sup>+</sup> T cells isolated from a previously described lean and obese cohort study.<sup>27</sup> As a reference, the subjects' demographic data and differences in BMI are shown in Supplementary Fig. 5A. Protein expression of FFAR2 was upregulated in the obese cohort (Supplementary Fig. 5B), which mirrors the relative expression of

the postfasting refeed state (Fig. 1C, D). As expected, the obese subjects' CD4<sup>+</sup> T cells expressed higher levels of genes encoding the T<sub>H</sub>1 and T<sub>H</sub>17 transcription factors with no difference in the T<sub>H</sub>2 transcription factor GATA3 (Supplementary Fig. 5C). In parallel, baseline secretion of canonical T<sub>H</sub>1 and T<sub>H</sub>17 cytokines was elevated in the obese subjects but not of IL-5 (T<sub>H</sub>2 cytokine) in response to TCR activation (Fig. 5A). Despite these different profiles, C3 blunted IFN $\gamma$  and IL-17 levels in the obese subjects and IFN $\gamma$  and IL-17 in the lean cohort (Fig. 5A). However, when assessing the degree of the effect of C3, the blunting of IFN $\gamma$  and IL-17 was significantly more robust in the obese vs lean cohorts (Fig. 5B). In parallel, we then functionally assessed whether the inflammatory cytokine release from CD4<sup>+</sup> T cells in the obese cohort was associated with increased FFAR2 levels. We found that IL-6 release from obese vs lean subject CD4<sup>+</sup> T cells was upregulated in baseline and that the FFAR2 antagonist GLPG0974 reversed the effect of C3 on blunting IL-6 release in both cohorts (Fig. 5C). Additionally, we showed that the FFAR2 agonist 4CMTB mirrored the blunting effect of C3 on CD4<sup>+</sup> T cell IL-6 release in both groups (Supplementary Fig. 5D).

## 4. Discussion

In this study, we find that propionate is unique among the SCFAs in that its levels are dynamically altered in response to prolonged fasting and refeeding. Serum propionate levels are increased with refeeding, and this is accompanied by increased expression in CD4<sup>+</sup> T cells of its cognate GPCRs, FFAR2 and FFAR3. Subsequent pharmacologic and genetic depletion studies support that propionate, via these GPCRs, downregulates transcripts

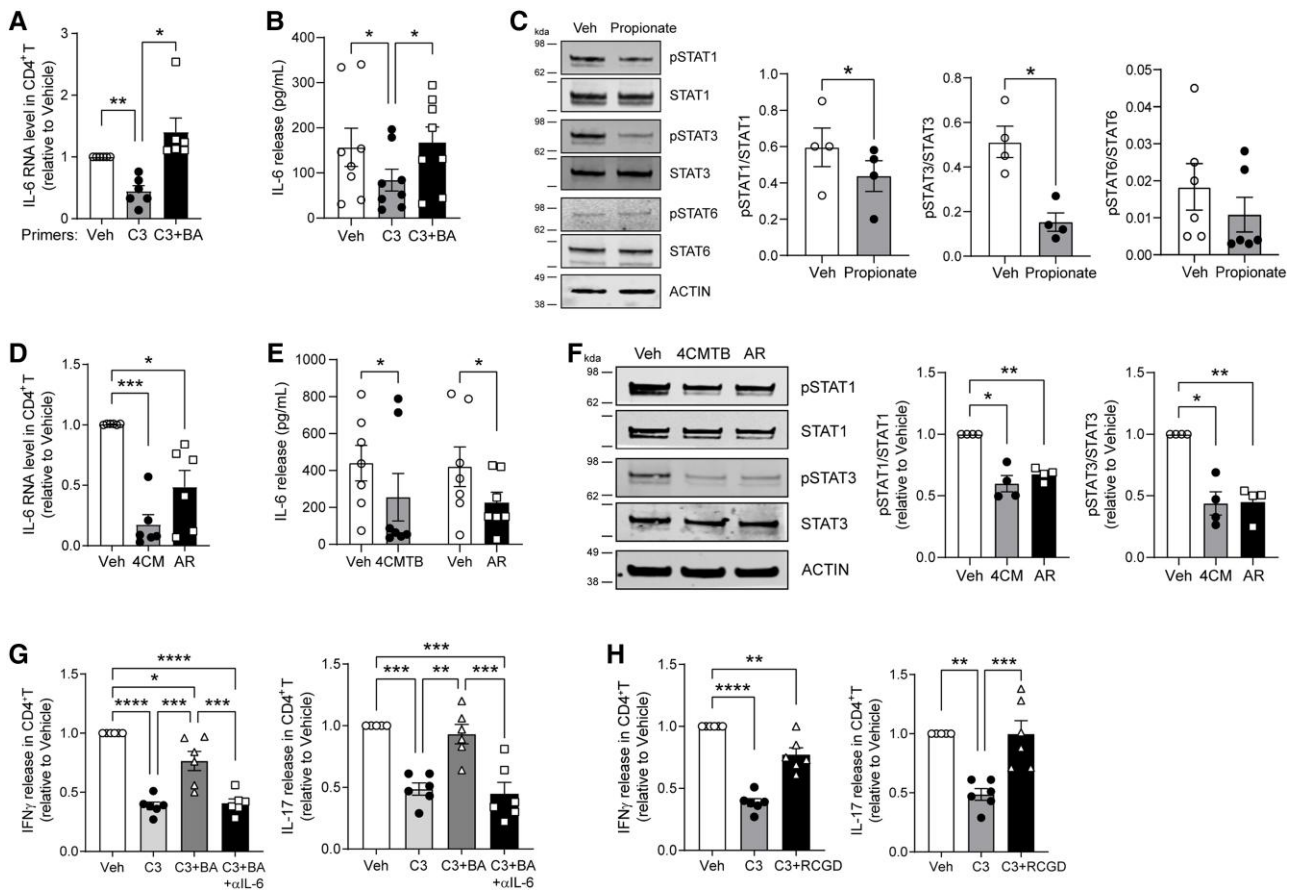


**Fig. 4.** Propionate regulates CD4<sup>+</sup> T cell activation by IL-6 through NF- $\kappa$ B signaling. (A) RNA expression of IL-6 in CD4<sup>+</sup> T cells treated with propionate (C3) and 10  $\mu$ M BA (NF- $\kappa$ B activator). RNA expression measured by quantitative real-time polymerase chain reaction and normalized to 18S and the mean of the vehicle group by  $\Delta\Delta$ Ct. Significance using a 1-way ANOVA with Šidák's multiple comparisons test. \* $P < 0.05$ , \*\* $P < 0.01$  ( $n = 6$ /group). (B) Release of IL-6 cytokine from CD4<sup>+</sup> T cells treated with C3 and BA. Significance using a 1-way ANOVA with Tukey's multiple comparisons test. \* $P < 0.05$  ( $n = 8$ ). (C) Immunoblot of STAT1, STAT3, and STAT6 protein and their phosphoprotein abundance in CD4<sup>+</sup> T cells treated with propionate. Quantification of immunoblot: pSTAT1/STAT1, pSTAT3/STAT3, and pSTAT6/STAT6 ( $n = 4-6$ ). Significance reported using a paired t test. \* $P < 0.05$ . (D) RNA expression of IL-6 in CD4<sup>+</sup> T cells treated with 4CMTB or AR. RNA expression measured by quantitative real-time polymerase chain reaction and normalized to 18S and the mean of the vehicle group by  $\Delta\Delta$ Ct. Significance using a 1-way ANOVA with Tukey's multiple comparisons test. \* $P < 0.05$ , \*\*\* $P < 0.001$  ( $n = 5-6$ /group). (E) IL-6 release from CD4<sup>+</sup> T cells treated with 4CMTB or AR. Significance reported using a paired t test. \* $P < 0.05$  ( $n = 5$ ). (F) Immunoblot image and quantification of pSTAT1 and pSTAT3 in FFAR2/FFAR3 agonist-treated CD4<sup>+</sup> T cells by TCR activation ( $n = 4$ ). Significance reported using a repeated measures 1-way ANOVA with Dunnett's multiple comparisons test. \* $P < 0.05$ , \*\* $P < 0.01$ . (G) Relative release of IFN $\gamma$  and IL-17 cytokines from CD4<sup>+</sup> T cells treated in combination with propionate, BA, and 1  $\mu$ g/mL IL-6-neutralizing antibodies ( $\alpha$ IL-6) compared with vehicle control ( $n = 5$ ). Significance reported using a repeated measures 1-way ANOVA with Tukey's multiple comparisons test. \* $P < 0.05$ , \*\* $P < 0.001$ , \*\*\* $P < 0.0001$ . (H) Relative release of IFN $\gamma$  and IL-17 cytokines from CD4<sup>+</sup> T cells treated in combination with propionate and 5  $\mu$ M RCGD423 (glycoprotein 130 [gp130] modulator) relative to vehicle control ( $n = 5$ ). Significance reported using a repeated measures 1-way ANOVA with Tukey's multiple comparisons test. \*\* $P < 0.01$ , \*\*\* $P < 0.001$ , \*\*\*\* $P < 0.0001$ . Veh = vehicle.

encoding T<sub>H</sub>1 and T<sub>H</sub>17 polarization regulatory transcription factors. Collectively, these lead to propionate-mediated blunting of IFN $\gamma$  and IL-17 secretion in response to TCR activation. Mechanistically, this propionate orchestrated pathway functions via inhibition of HDAC activity and the subsequent downregulation of NF $\kappa$ B-IL6 orchestrated STAT1 and STAT3 activation. Subsequent data in different cohorts support that this metabolite-initiated pathway may be operational in older lean and obese individuals. Overall, these findings expand our understanding of how human dietary interventions modulate the SCFA propionate and how this can have acute regulatory effects on circulating CD4<sup>+</sup> T<sub>H</sub> cells.

Recognition of the role of the gut microbiome's interaction with the host via SCFA production and signaling is rapidly expanding.<sup>37</sup> Within the gut, propionate confers anti-inflammatory effects.<sup>38</sup> With respect to its systemic role, propionate is transported through the portal vein to the liver, where it functions as a

precursor for hepatic protein synthesis, gluconeogenesis, and liponeogenesis, with a smaller proportion being released into the circulation.<sup>39</sup> As a systemic signaling metabolite, propionate has a myriad of effects, including anti-inflammatory effects, as described previously.<sup>23-26</sup> Interestingly, data are emerging that intermittent fasting and fasting-mimicking diets increase the gut microbiome population of *Akkermansia muciniphila*, which are known to synthesize propionate.<sup>40,41</sup> In parallel, these restrictive caloric interventions have been shown to confer anti-inflammatory effects. However, these were longer-term studies spanning over 10 d or more, which contrasts with our acute fasting and refeeding intervention.<sup>42</sup> At the same time, it is interesting that circulating propionate levels observed were higher in the refeed state. Whether this is delayed release into the circulation or implicates a novel aspect of refeeding following a 24-h fast will need to be determined. Moreover, whether this acute intervention modulates the gut microbiome to increase propionate



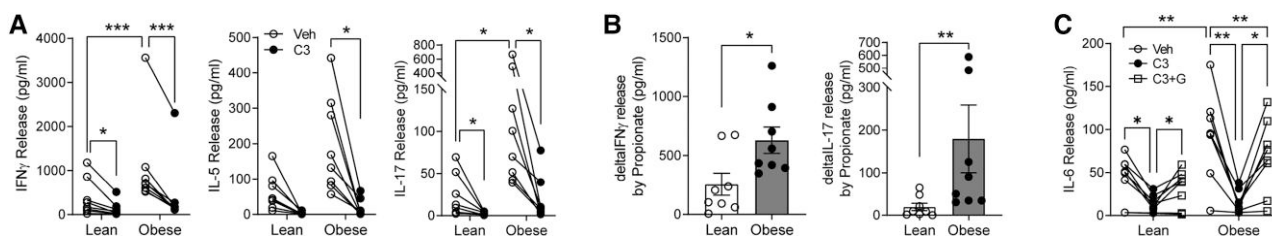


**Fig. 5.** Anti-inflammatory effects of propionate are operational in obesity. (A) Release of IFN $\gamma$ , IL-5, and IL-17 cytokines from CD4<sup>+</sup> T cells isolated from lean or obese volunteers and treated with propionate or vehicle control (n = 8). Cytokines measured by ELISA immunoassay and normalized to cell density by CyQuant assay. Significance reported using a 2-way ANOVA with Turkey's multiple comparisons test. \*P < 0.05, \*\*\*P < 0.001. (B) Differential cytokine level downregulated by propionate in lean and obese subjects (n = 8). Significance reported using an unpaired Mann-Whitney test. \*P < 0.05, \*\*P < 0.01. (C) IL-6 cytokine release from CD4<sup>+</sup> T cells treated with C3 and FFAR2 antagonist, GLPG0974 (G). Significance reported using a 2-way ANOVA with Turkey's multiple comparisons test (n = 8). \*P < 0.05, \*\*P < 0.01.

production would need to be directly validated. The finding that propionate modulates the levels of FFARs and transcripts encoding FFARs are modulated by fasting and refeeding would support relatively rapid regulation of these signaling events. At the same time, it is interesting that the snapshot in time analysis showed that FFAR2 levels in CD4<sup>+</sup> T cells increased in obese subjects. Whether this reflects counterregulatory control to attenuate the basal inflammation associated with obesity would be an interesting concept to explore further.

A previous study found propionate could reduce IL-17 release from mouse intestinal  $\gamma\delta$  T cells by inhibiting HDAC.<sup>23</sup> The HDAC inhibitor TSA could replicate the anti-inflammatory effects of propionate on  $\gamma\delta$  T cells and had no additive effects when used in combination with propionate.<sup>23</sup> We further validated that propionate blunted HDAC activity, linking gene expression to inflammatory signaling via NF- $\kappa$ B downstream of CD4<sup>+</sup> T cell differentiation and activation.<sup>43,44</sup>

The concept that refeeding initiates a proinflammatory milieu is well established in murine studies and human health and disease.<sup>2,5,45</sup> The mechanisms are being explored in different model systems and for different cell lineages. These include fasting and refeeding effects on the hypothalamic-pituitary-adrenal axis,<sup>5</sup> hepatic AMPK and PPAR $\alpha$  activity,<sup>11</sup> and evidence of putative refeeding-associated intestinal tract endotoxin leak into the circulation.<sup>1</sup> Some of these changes may also be operational in chronic dietary conditions, in that evidence of endotoxemia is elevated in obesity,<sup>46</sup> and 4 weeks of a caloric restriction diet in obese subjects blunts this effect.<sup>47</sup> At the same time, the concept that circulating metabolites themselves can have immunoregulatory effects is actively being explored, as described previously. However, the finding that an SCFA, i.e. propionate, via its GPCR could have a counterregulatory effect to ameliorate the refeeding "proinflammatory milieu" is a new and interesting observation.

The effect of dietary composition on propionate levels has also been examined, with extensive data linking dietary fiber fermentation to gut microbial production of SCFA.<sup>48,49</sup> Moreover, in comparing a prior obese to lean cohort, the dietary fiber intake was reduced, in parallel with lower serum levels of propionate, despite no differences in the levels of butyrate or acetate with obesity.<sup>50</sup> Furthermore, and consistent with the concept that obesity triggers inflammation, serum lipopolysaccharide levels were concurrently shown to be higher in this obese compared with lean cohort.<sup>50</sup> Participants in this fasting and refeeding study included an isocaloric choice of egg-based (5.6 g total fiber) or oatmeal-based (5.9 g total fiber) breakfasts as the refed meal.<sup>2</sup> Interestingly, the induction of propionate levels with refeeding was more pronounced with the lower fiber (egg-based) meal.

The difference in fiber content in this study is modest (5.3%), and the number of subjects in this exploratory study is limited, precluding the ability to make any firm conclusions from these data. However, the lack of correlation between fiber content and change in propionate levels raises questions about whether dietary composition is a major component in the change in propionate levels and/or whether different dietary components play a role in this biology. Nevertheless, whether the elevation of propionate could be due to the acute dietary intervention alone and/or is a consequence of microbiome effects from the fasting intervention needs to be evaluated further.

One limitation of the study is that the dynamic changes in propionate levels at different times in the fasting refeeding continuum were not assessed. Exploring this in the future may give even greater insight into the regulatory role of this SCFA on CD4<sup>+</sup> T cell immunity. Furthermore, in the lean and obese populations, blood was drawn after an overnight fast. The levels of SCFAs in the fasting-refeeding continuum have the potential to be more revealing and should be investigated further. At the same time, it is interesting that the different FFAR agonists appear to function in distinct ways, i.e. as either an allosteric agonist and/or via gene regulatory effects that modulate the receptor expression. These distinct mechanisms additionally require further study. Finally, this study employed a reductionist approach to evaluate the effects of propionate levels on CD4<sup>+</sup> T cell biology. With advancing technological sensitivity and lipidomic studies, directly annotating SCFA levels linked to inflammatory diseases may give us additional insight into this biology.

In conclusion, this study expands our understanding of the role of propionate in circulating CD4<sup>+</sup> T cell regulation. Furthermore, it uncovers that circulating propionate levels can modulate the expression of its cognate GPCRs in CD4<sup>+</sup> T cells and that this metabolite is unique among SCFAs in its dynamic change in levels in response to fasting and refeeding. Finally, these data suggest that propionate can confer a counterregulatory effect to blunt CD4<sup>+</sup> T cell responsiveness within the context of the proinflammatory nutrient milieu of refeeding and potentially in obesity.

## Acknowledgments

The authors thank Drs. Antonio Murgia and Ben McNally of the University of Cambridge Biochemistry Department for their contributions to metabolomics and lipidomic data processing. They thank and acknowledge the assistance of the National Heart, Lung, and Blood Institute DNA Sequencing and Genomics Core in performing the RNA library sequencing and the National Heart, Lung, and Blood Institute Flow Cytometry Core for performing the flow cytometry.

## Author contributions

K.H., A.M.M., M.J.R., J.L.G., and M.N.S. conceived this study. K.H., A.M.M., M.J.R., A.C.R., R.S., S.H., P.K.D., F.N.K., J.L.G., and M.N.S. performed experiments and analyzed the data. R.D.H., T.M.P-W., and Y.B. supported the resources. K.H., A.M.M., K.S., Y.B., J.L.G., and M.N.S. carried out manuscript writing and editing. J.L.G. and M.N.S. supervised experiments and secured funding for this study.

## Supplementary material

Supplementary materials are available at *Journal of Leukocyte Biology* online.

## Funding

This research was supported by the National Institute of Heart, Lung, and Blood Institute Division of Intramural Research (MNS-HL005199) and the Medical Research Council of the United Kingdom (JLG—MR/P011705/2; UKDRI-5002; MAP UK).

Conflict of interest statement. None declared.

## References

- Traba J, Kwarteng-Siaw M, Okoli TC, Li J, Huffstutler RD, Bray A, Waclawiw MA, Han K, Pelletier M, Sauve AA, et al. Fasting and re-feeding differentially regulate NLRP3 inflammasome activation in human subjects. *J Clin Invest*. 2015;125(12):4592–4600. <https://doi.org/10.1172/JCI83260>
- Han K, Singh K, Rodman MJ, Hassanzadeh S, Wu K, Nguyen A, Huffstutler RD, Seifuddin F, Dagur PK, Saxena A, et al. Fasting-induced FOXO4 blunts human CD4(+) T helper cell responsiveness. *Nat Metab*. 2021;3(3):318–326. <https://doi.org/10.1038/s42255-021-00356-0>
- Meydani SN, Das SK, Pieper CF, Lewis MR, Klein S, Dixit VD, Gupta AK, Villareal DT, Bhapkar M, Huang M, et al. Long-term moderate calorie restriction inhibits inflammation without impairing cell-mediated immunity: a randomized controlled trial in non-obese humans. *Aging (Albany NY)*. 2016;8(7):1416–1431. <https://doi.org/10.18632/aging.100994>
- Spadaro O, Youm Y, Shchukina I, Ryu S, Sidorov S, Ravussin A, Nguyen K, Aladyeva E, Predeus AN, Smith SR, et al. Caloric restriction in humans reveals immunometabolic regulators of health span. *Science*. 2022;375(6581):671–677. <https://doi.org/10.1126/science.abg7292>
- Janssen H, Kahles F, Liu D, Downey J, Koekkoek LL, Roudko V, D'Souza D, McAlpine CS, Halle L, Poller WC, et al. Monocytes re-enter the bone marrow during fasting and alter the host response to infection. *Immunity*. 2023;56(4):783–796.e7. <https://doi.org/10.1016/j.immuni.2023.01.024>
- Roy DG, Chen J, Mamane V, Ma EH, Muhire BM, Sheldon RD, Shorstova T, Koning R, Johnson RM, Esaulova E, et al. Methionine metabolism shapes T helper cell responses through regulation of epigenetic reprogramming. *Cell Metab*. 2020;31(2):250–266.e9. <https://doi.org/10.1016/j.cmet.2020.01.006>
- Chen X, Lu Y, Zhang Z, Wang J, Yang H, Liu G. Intercellular interplay between sirt1 signalling and cell metabolism in immune cell biology. *Immunology*. 2015;145(4):455–467. <https://doi.org/10.1111/imm.12473>
- Palma C, La Rocca C, Gigantino V, Aquino G, Piccaro G, Di Silvestre D, Brambilla F, Rossi R, Bonacina F, Lepore MT, et al. Caloric restriction promotes immunometabolic reprogramming leading to protection from tuberculosis. *Cell Metab*. 2021;33(2):300–318.e12. <https://doi.org/10.1016/j.cmet.2020.12.016>
- Wagner A, Wang C, Fessler J, DeTomaso D, Avila-Pacheco J, Kaminski J, Zaghouni S, Christian E, Thakore P, Schellhaass B, et al. Metabolic modeling of single Th17 cells reveals regulators of autoimmunity. *Cell*. 2021;184(16):4168–4185.e21. <https://doi.org/10.1016/j.cell.2021.05.045>
- Han K, Singh K, Rodman MJ, Hassanzadeh S, Baumer Y, Huffstutler RD, Chen J, Candia J, Cheung F, Stagliano KER, et al. Identification and validation of nutrient state-dependent Serum protein mediators of human CD4(+) T cell responsiveness. *Nutrients*. 2021;13(5):1492. <https://doi.org/10.3390/nu13051492>
- Jordan S, Tung N, Casanova-Acebes M, Chang C, Cantoni C, Zhang D, Wirtz TH, Naik S, Rose SA, Brocker CN, et al. Dietary intake regulates the circulating inflammatory monocyte pool. *Cell*. 2019;178(5):1102–1114.e17. <https://doi.org/10.1016/j.cell.2019.07.050>
- Fazeli PK, Bredella MA, Pachon-Pena G, Zhao W, Zhang X, Faje AT, Resulaj M, Polineni SP, Holmes TM, Lee H, et al. The dynamics of human bone marrow adipose tissue in response to feeding and fasting. *JCI Insight*. 2021;6(12):e138636. <https://doi.org/10.1172/jci.insight.138636>
- Maifeld A, Bartolomeaus H, Lober U, Avery EG, Steckhan N, Marko L, Wilck N, Hamad I, Susnjar U, Mahler A, et al. Fasting alters the gut microbiome reducing blood pressure and body weight in metabolic syndrome patients. *Nat Commun*. 2021;12(1):1970. <https://doi.org/10.1038/s41467-021-22097-0>
- Nagai M, Noguchi R, Takahashi D, Morikawa T, Koshida K, Komiyama S, Ishihara N, Yamada T, Kawamura YI, Muroi K, et al. Fasting-Refeeding impacts immune cell dynamics and mucosal immune responses. *Cell*. 2019;178(5):1072–1087.e14. <https://doi.org/10.1016/j.cell.2019.07.047>
- Youm YH, Nguyen KY, Grant RW, Goldberg EL, Bodogai M, Kim D, D'Agostino D, Planavsky N, Lupfer C, Kanneganti TD, et al. The ketone metabolite beta-hydroxybutyrate blocks NLRP3 inflammasome-mediated inflammatory disease. *Nat Med*. 2015;21(3):263–269. <https://doi.org/10.1038/nm.3804>
- Goldberg EL, Letian A, Dlugos T, Leveau C, Dixit VD. Innate immune cell-intrinsic ketogenesis is dispensable for organismal metabolism and age-related inflammation. *J Biol Chem*. 2023;299(3):103005. <https://doi.org/10.1016/j.jbc.2023.103005>
- Martensson J, Bjorkman L, Lind S, Viklund MB, Zhang L, Gutierrez S, Dahlgren C, Sundqvist M, Xie X, Forsman H. The ketone body acetoacetate activates human neutrophils through FFAR2. *J Leukoc Biol*. 2023;113(6):577–587. <https://doi.org/10.1093/jleuko/qiad035>
- Wu XJ, Shu QQ, Wang B, Dong L, Hao B. Acetoacetate improves memory in Alzheimer's mice via promoting brain-derived neurotrophic factor and inhibiting inflammation. *Am J Alzheimers Dis Other Demen*. 2022;37:15333175221124949. <https://doi.org/10.1177/15333175221124949>
- Onizawa Y, Katoh T, Miura R, Konda K, Noguchi T, Iwata H, Kuwayama T, Hamano S, Shirasuna K. Acetoacetate is a trigger of NLRP3 inflammasome activation in bovine peripheral blood mononuclear cells. *Vet Immunol Immunopathol*. 2022;244:110370. <https://doi.org/10.1016/j.vetimm.2021.110370>
- Ratajczak W, Ryl A, Mizerski A, Walczakiewicz K, Sipak O, Laszczynska M. Immunomodulatory potential of gut microbiome-derived short-chain fatty acids (SCFAs). *Acta Biochim Pol*. 2019;66(1):1–12. [https://doi.org/10.18388/abp.2018\\_2648](https://doi.org/10.18388/abp.2018_2648)
- Chriett S, Dabek A, Wojtala M, Vidal H, Balcerczyk A, Pirola L. Prominent action of butyrate over beta-hydroxybutyrate as histone deacetylase inhibitor, transcriptional modulator and anti-

- inflammatory molecule. *Sci Rep.* 2019;9(1):742. <https://doi.org/10.1038/s41598-018-36941-9>
22. Wang X, He G, Peng Y, Zhong W, Wang Y, Zhang B. Sodium butyrate alleviates adipocyte inflammation by inhibiting NLRP3 pathway. *Sci Rep.* 2015;5(1):12676. <https://doi.org/10.1038/srep12676>
  23. Dupraz L, Magniez A, Rolhion N, Richard ML, Da Costa G, Touch S, Mayeur C, Planchais J, Agus A, Danne C, et al. Gut microbiota-derived short-chain fatty acids regulate IL-17 production by mouse and human intestinal gammadelta T cells. *Cell Rep.* 2021;36(1):109332. <https://doi.org/10.1016/j.celrep.2021.109332>
  24. Duscha A, Gisevius B, Hirschberg S, Yissachar N, Stangl GI, Eilers E, Bader V, Haase S, Kaisler J, David C, et al. Propionic acid shapes the multiple sclerosis disease course by an immunomodulatory mechanism. *Cell.* 2020;180(6):1067–1080.e16. <https://doi.org/10.1016/j.cell.2020.02.035>
  25. Haase S, Maurer J, Duscha A, Lee DH, Balogh A, Gold R, Muller DN, Haghikia A, Linker RA. Propionic acid rescues high-fat diet enhanced immunopathology in autoimmunity via effects on Th17 responses. *Front Immunol.* 2021;12:701626. <https://doi.org/10.3389/fimmu.2021.701626>
  26. Haselbarth L, Ouwens DM, Teichweyde N, Hochrath K, Merches K, Esser C. The small chain fatty acid butyrate antagonizes the TCR-stimulation-induced metabolic shift in murine epidermal gamma delta T cells. *EXCLI J.* 2020;19:334–350. <https://doi.org/10.17179/excli2020-1123>
  27. Meadows AM, Han K, Singh K, Murgia A, McNally BD, West JA, Huffstutler RD, Powell-Wiley TM, Baumer Y, Griffin JL, et al. N-arachidonylglycine is a caloric state-dependent circulating metabolite which regulates human CD4(+)T cell responsiveness. *iScience.* 2023;26(5):106578. <https://doi.org/10.1016/j.isci.2023.106578>
  28. Le Belle JE, Harris NG, Williams SR, Bhakoo KK. A comparison of cell and tissue extraction techniques using high-resolution 1H-NMR spectroscopy. *NMR Biomed.* 2002;15(1):37–44. <https://doi.org/10.1002/nbm.740>
  29. Han J, Lin K, Sequeira C, Borchers CH. An isotope-labeled chemical derivatization method for the quantitation of short-chain fatty acids in human feces by liquid chromatography-tandem mass spectrometry. *Anal Chim Acta.* 2015;854:86–94. <https://doi.org/10.1016/j.aca.2014.11.015>
  30. Li M, van Esch B, Henricks PAJ, Folkerts G, Garssen J. The anti-inflammatory effects of short chain fatty acids on lipopolysaccharide- or tumor necrosis factor alpha-stimulated endothelial cells via activation of GPR41/43 and inhibition of HDACs. *Front Pharmacol.* 2018;9:533. <https://doi.org/10.3389/fphar.2018.00533>
  31. Glauben R, Sonnenberg E, Wetzell M, Mascagni P, Siegmund B. Histone deacetylase inhibitors modulate interleukin 6-dependent CD4+ T cell polarization in vitro and in vivo. *J Biol Chem.* 2014;289(9):6142–6151. <https://doi.org/10.1074/jbc.M113.517599>
  32. Place RF, Noonan EJ, Giardina C. HDAC inhibition prevents NF-kappa B activation by suppressing proteasome activity: down-regulation of proteasome subunit expression stabilizes I kappa B alpha. *Biochem Pharmacol.* 2005;70(3):394–406. <https://doi.org/10.1016/j.bcp.2005.04.030>
  33. Hu X, Li J, Fu M, Zhao X, Wang W. The JAK/STAT signaling pathway: from bench to clinic. *Signal Transduct Target Ther.* 2021;6(1):402. <https://doi.org/10.1038/s41392-021-00791-1>
  34. O'Shea JJ, Lahesmaa R, Vahedi G, Laurence A, Kanno Y. Genomic views of STAT function in CD4+ T helper cell differentiation. *Nat Rev Immunol.* 2011;11(4):239–250. <https://doi.org/10.1038/nri2958>
  35. Winer S, Chan Y, Paltser G, Truong D, Tsui H, Bahrami J, Dorfman R, Wang Y, Zielinski J, Mastrorandi F, et al. Normalization of obesity-associated insulin resistance through immunotherapy. *Nat Med.* 2009;15(8):921–929. <https://doi.org/10.1038/nm.2001>
  36. Winer S, Paltser G, Chan Y, Tsui H, Engleman E, Winer D, Dosch HM. Obesity predisposes to Th17 bias. *Eur J Immunol.* 2009;39(9):2629–2635. <https://doi.org/10.1002/eji.200838893>
  37. Sanna S, van Zuydam NR, Mahajan A, Kurilshikov A, Vich Vila A, Vosa U, Mujagic Z, Masclee AAM, Jonkers D, Oosting M, et al. Causal relationships among the gut microbiome, short-chain fatty acids and metabolic diseases. *Nat Genet.* 2019;51(4):600–605. <https://doi.org/10.1038/s41588-019-0350-x>
  38. Bajic D, Niemann A, Hillmer AK, Mejias-Luque R, Bluemel S, Docampo M, Funk MC, Tonin E, Boutros M, Schnabl B, et al. Gut Microbiota-derived propionate regulates the expression of reg3 mucosal lectins and ameliorates experimental colitis in mice. *J Crohns Colitis.* 2020;14(10):1462–1472. <https://doi.org/10.1093/ecco-jcc/jjaa065>
  39. Murugesan S, Nirmalkar K, Hoyo-Vadillo C, Garcia-Espitia M, Ramirez-Sanchez D, Garcia-Mena J. Gut microbiome production of short-chain fatty acids and obesity in children. *Eur J Clin Microbiol Infect Dis.* 2018;37(4):621–625. <https://doi.org/10.1007/s10096-017-3143-0>
  40. Rangan P, Choi I, Wei M, Navarrete G, Guen E, Brandhorst S, Enyati N, Pasia G, Maesincee D, Ocon V, et al. Fasting-Mimicking diet modulates Microbiota and promotes intestinal regeneration to reduce inflammatory bowel disease pathology. *Cell Rep.* 2019;26(10):2704–2719.e6. <https://doi.org/10.1016/j.celrep.2019.02.019>
  41. Su J, Braat H, Peppelenbosch MP. Gut Microbiota-derived propionate production may explain beneficial effects of intermittent fasting in experimental colitis. *J Crohns Colitis.* 2021;15(6):1081–1082. <https://doi.org/10.1093/ecco-jcc/jjaa248>
  42. Fazeli PK, Zhang Y, O'Keefe J, Pesaresi T, Lun M, Lawney B, Steinhauser ML. Prolonged fasting drives a program of metabolic inflammation in human adipose tissue. *Mol Metab.* 2020;42:101082. <https://doi.org/10.1016/j.molmet.2020.101082>
  43. Bartolomaeus H, Balogh A, Yakoub M, Homann S, Marko L, Hoges S, Tsvetkov D, Krannich A, Wundersitz S, Avery EG, et al. Short-Chain fatty acid propionate protects from hypertensive cardiovascular damage. *Circulation.* 2019;139(11):1407–1421. <https://doi.org/10.1161/CIRCULATIONAHA.118.036652>
  44. Deng M, Qu F, Chen L, Liu C, Zhang M, Ren F, Guo H, Zhang H, Ge S, Wu C, et al. SCFAs alleviated steatosis and inflammation in mice with NASH induced by MCD. *J Endocrinol.* 2020;245(3):425–437. <https://doi.org/10.1530/JOE-20-0018>
  45. Han K, Nguyen A, Traba J, Yao X, Kaler M, Huffstutler RD, Levine SJ, Sack MN. A pilot study to investigate the immune-modulatory effects of fasting in steroid-naive mild asthmatics. *J Immunol.* 2018;201(5):1382–1388. <https://doi.org/10.4049/jimmunol.1800585>
  46. Sun L, Yu Z, Ye X, Zou S, Li H, Yu D, Wu H, Chen Y, Dore J, Clement K, et al. A marker of endotoxemia is associated with obesity and related metabolic disorders in apparently healthy Chinese. *Diabetes Care.* 2010;33(9):1925–1932. <https://doi.org/10.2337/dc10-0340>
  47. Ott B, Skurk T, Hastreiter L, Lagkouvardos I, Fischer S, Buttner J, Kellerer T, Clavel T, Rychlik M, Haller D, et al. Effect of caloric restriction on gut permeability, inflammation markers, and fecal microbiota in obese women. *Sci Rep.* 2017;7(1):11955. <https://doi.org/10.1038/s41598-017-12109-9>
  48. Cummings JH, Pomare EW, Branch WJ, Naylor CP, Macfarlane GT. Short chain fatty acids in human large intestine, portal, hepatic and venous blood. *Gut.* 1987;28(10):1221–1227. <https://doi.org/10.1136/gut.28.10.1221>



49. Gill PA, van Zelm MC, Muir JG, Gibson PR. Review article: short chain fatty acids as potential therapeutic agents in human gastrointestinal and inflammatory disorders. *Aliment Pharmacol Ther.* 2018;48(1):15–34. <https://doi.org/10.1111/apt.14689>
50. Nabil LM, Sallam MM, Mohamed DAW, Salib MM, Abdelsalam HM, Sallam RM. Healthy dietary choices are associated with higher serum propionate and PGC1 $\alpha$  expression in peripheral blood mononuclear cells in adult humans. *Obes Med.* 2022;33:100432. <https://doi.org/10.1016/j.obmed.2022.100432>